Radiation Physics and Chemistry 204 (2023) 110676

Contents lists available at ScienceDirect

Radiation Physics and Chemistry

journal homepage: www.elsevier.com/locate/radphyschem

Nuclear radiation shielding performance of borosilicate glasses: Numerical simulations and theoretical analyses

O. Kilicoglu [a,b,*], F. Akman [c,d], H. Ogul [e], O. Agar [f], U. Kara [g]

[a] *Vocational School of Health Services, Marmara University, Kartal, Istanbul, Turkey*
[b] *Radiation Laboratory, University of Notre Dame, Notre Dame, IN, 46556-5670, USA*
[c] *Bingöl University, Central Laboratory Application and Research Center, 12000, Bingöl, Turkey*
[d] *Bingöl University, Vocational School of Social Sciences, Department of Property Protection and Security, Program of Occupational Health and Safety, 12000, Bingöl, Turkey*
[e] *Department of Nuclear Engineering, Faculty of Engineering and Architecture, Sinop University, Sinop, Turkey*
[f] *Karamanoğlu Mehmetbey University, Department of Medical Imaging Techniques, 70100, Karaman, Turkey*
[g] *Medical Imaging Department, Vocational School of Health Services, Suleyman Demirel University, Isparta, Turkey*

A R T I C L E I N F O

Keywords:
Borosilicate
Radiation shielding
FLUKA
GEANT4
MATLAB
Buildup factor

A B S T R A C T

The photon shielding performances of five different borosilicate-based glasses were investigated in this study using the FLUKA, GEANT4 and MATLAB codes, as well as the XCOM program, at photon energies ranging from 0.03 to 15 MeV. In this context, dependencies of the photon attenuation features with the variation of the photon energy and the chemical compositions have been carefully evaluated with Monte Carlo simulation and theoretical evaluation tools. The mass attenuation coefficient values and effective atomic numbers obtained for BaO-doped G5 glasses are found to be higher than those derived for G1-G4 samples. In other words, the Z_{eff} results showed that high Z-elements such as Ba in a suitable amount should be inserted into the glass composition in order to improve the photon attenuation capability of the borosilicate glasses. The HVLs, TVLs, and MFPs of the studied borosilicate glasses are determined further, and the gamma shielding characteristics of the analyzed samples are found to be associated to the density of the glass, implying that high-density glass can be used for high-level attenuation performance. The exposure buildup factor (EBF) values have been further estimated via the G-P fitting approach. The results of such investigations, according to the work given, may be valuable in designing and fabricating new borosilicate-based glasses, which can then shield against potential radiation damage to environmental health.

1. Introduction

Advanced electronic devices in some fields such as aerospace and nuclear technology, and many scientific and medical equipment are utilized under the impact of a wide range of high energetic nuclear ionizing radiations (Tishkevich et al., 2018, 2020). In the long run, it can cause defects in the operation of such systems, which is related to the radiation effects occurrence in integrated circuits. Because high-density materials are ideal for radiation protection, lead (Pb) or Pb-containing concretes, alloys, and composites are commonly used in radiation protection applications. However, Pb, which is known to have a large toxic effect, can easily enter the human body through digestion and inhalation, and unfortunately, the excretion of the absorbed Pb from the body is quite slow. It could be mixed with the blood over time and distributed to the body through blood circulation. Besides, there are further disadvantages of the use Pb element such as its damage on the hematopoietic system, central nervous system, peripheral nerves and kidneys. In short, its usage could cause many health problems in adults, children and pregnant women. Nevertheless, Pb or Pb-based materials has been used in many fields, and the search for alternative materials, especially in the field of radiation shielding, has been accelerated in recent years. Based on the intended usage area of the shielding application, the preferred and developed shielding material differs since each type offers different and unique advantages to its users. The main studied material types in this context are Pb-free composites (Cherkashina et al., 2019; More et al., 2021; Ferdi Akman et al., 2021) alloys (Tekin and Kilicoglu, 2020; Tellili et al., 2017; F. Akman et al., 2019), ceramics (Kacal et al., 2019; Oto et al., 2019), concretes (Azeez et al., 2019; Baalamurugan et al.,

* Corresponding author. Vocational School of Health Services, Marmara University, Kartal, Istanbul, Turkey.
E-mail address: ozgekoglu@gmail.com (O. Kilicoglu).

https://doi.org/10.1016/j.radphyschem.2022.110676
Received 29 August 2022; Received in revised form 23 October 2022; Accepted 26 November 2022
Available online 1 December 2022

2019; Alwaeli, 2017) and glasses (Issa et al., 2019; Tijani et al., 2018; Boukhris et al., 2020).

Due to its distinctive advantages, glasses are chosen in the roentgen, mammography, and bone densitometry areas of hospitals. Some of these advantages stand out as their excellent light transmission, low thermal and electrical conductivity, not being affected by corrosion, and pressure and tensile strength. Before going deeper discussion on gamma radiation shielding, it should be noted here that the preferred glass type in laboratories and places, where conditions are hard, is borosilicate-based glasses, consist of silica and boron trioxide, while most of the glasses in our daily life are soda-lime-based glasses. Soda-lime or soda-lime-silica glasses are the most common glass type since they are used in window glasses and in bottles and jars of many commercial products. On the other hand, the main motivation on preferring borosilicate-based glasses is the fact that they show good thermal, mechanical and chemical properties compared to soda-lime-based glasses. In essence, the borosilicate-based glasses possess high thermal resistance and low thermal expansion coefficients. Here, it should be underlined that a lower linear thermal expansion coefficient makes borosilicate glass more resistant to thermal shock compare to soda-lime glass. In addition, borosilicate glass is harder and more resistant to acids than soda-lime glass. These unique properties of borosilicated glasses motivated their usage in radiation shielding applications and some studies have been performed in recent years. This have opened an alternative usage area for the motivated borosilicated glasses. In terms of radiation shielding, both borosilicate-based glasses and soda-lime-based glasses contain different elements or compounds in different proportions. In one of the recent borosilicate glass study, Kurtulus et al. added Bi_2O_3 at different ratios into alumino-borosilicate-based glasses and investigated gamma attenuation properties of the prepared samples (Kurtulus et al., 2021). They reported a good indication of borosilicate-based glasses on gamma radiation shielding. In another study, Zakaly et al. doped BaO into borosilicate-based glasses, and they concluded that the increase of Ba content improved the radiation attenuation capability of borosilicate glasses (Zakaly et al., 2021). Besides, Al-Hadeethi and Sayyed studied borosilicate-based glasses including different proportions of Bi_2O_3, BaO and TiO_2 (Al-Hadeethi and Sayyed, 2019). The shielding tests showed that addition of TiO_2, BaO and Bi_2O_3 enhanced the gamma radiation shielding property. Similarly, Ruengsri et al. prepared borosilicate glass samples containing BaO and reported the improved radiation attenuation ability and optical transparency for the borosilicate glasses (Ruengsri et al., 2015). Additionally, Sangwaranatee et al. investigated the radiation shielding properties for alumino-borosilicate-based glasses by adding Bi_2O_3 at different energies and observed a linear relationship between the amount of doping and radiation shielding properties (Sangwaranatee et al., 2021). In another reported work, Kurudirek et al. investigated the radiation shielding properties of the recycled borosilicate glasses from high-pressure sodium lamps and the glass samples obtained by adding different ratios of Bi_2O_3 at 0.662, 1.173 and 1.332 MeV photon energies (Kurudirek et al., 2018). They reported that gamma and fast neutron shielding properties improved with increasing Bi_2O_3 ratio. Kavaz et al. investigated the radiation shielding capacities of window, PbO, soda and borosilicate glasses in the energy range of 0.015–15 MeV and reported that PbO glass showed the best radiation shielding among them (Kavaz et al., 2019). On the other hand, gamma-ray exposure buildup factors and neutron shielding capacities of Bi_2O_3 doped borosilicate glasses have investigated by Singh et al. and they noted that the shielding properties improved with increasing Bi_2O_3 (V. P. Singh et al., 2014). In other work, Kurtulus et al. soda-lime-silica-based glasses doped with Bi_2O_3 and Sb_2O_3 at different ratios (Kurtulus et al., 2020), Sayyed et al. soda-lime-silica-based glasses with different ratios of Sb_2O_3 and ZnO (Sayyed et al., 2020), and Kavas et al. investigated the ionizing radiation shielding properties of soda-lime-silica-based glasses doped with Ta_2O_5 at different ratios and different energies (Kavas et al., 2021). All noted that the shielding properties improved with increasing doping amount. Besides, Akkurt et al. investigated the radiation shielding properties of soda-lime-based and La_2O_3 doped glasses at different ratios with the help of a NaI(Tl) detector at 511 and 1275 keV photon energies, and reported that the glass sample with the highest doped ratio (0.5 wt%) is the best radiation shielding material (Akkurt et al., 2021).

The feasibility of various undoped daily or waste glasses as a nuclear radiation shield could be extremely significant to investigate the comprehensive shielding behaviors of such glasses. In this study, the mass attenuation coefficients (MAC), half value layers (HVL), tenth value layers (TVL), mean free path (MFP), and effective atomic numbers (Zeff) of expansion borosilicate, borosilicate (clear), borosilicate (amber), expansion soda-lime (clear), and expansion soda-lime (amber) glasses were calculated in the photon energy range of 0.03–15 MeV. The calculations were carried out through MATLAB, GEANT4 and FLUKA codes as well as XCOM program, and the obtained results were compared with each other. Finally, Exposure buildup factors (EBF) in the energy range of 0.03–15 MeV at different penetration depths (1–15 MFP) were calculated.

2. Materials and method

2.1. Theoretical basis

Linear attenuation coefficient (LAC, μ) is described as a measure of radiation density reduction caused by the interaction of photons emitted from the radiaoctive source with the material and can be estimated utilizing Beer-Lambert equation (Kilicoglu, 2019):

$$\mu = -\frac{\ln\frac{I}{I_0}}{x} \tag{2}$$

where I_0 and I photon intensities are "un-attenuated" and "attenuated" measurements, respectively, x denote thickness of the sample.

The accuracy of the designed scheme and photon attenuation of the absorber can be approved via well-known mixture rule (Limkitjaroenporn et al., 2011; Tekin and Kilicoglu, 2020):

$$\mu_m = \frac{\mu}{\rho} = \sum w_i \left(\frac{\mu}{\rho}\right)_i \tag{3}$$

where μ_m and ρ show the mass attenuation coefficients (MAC,$cm^2\ g^{-1}$) and the density ($g\ cm^{-3}$) of the absorber, respectively.

The quantity which needs to be carefully investigated before the application of any absorber is effective atomic number (Z_{eff}) and can be obtained using MAC values (Tekin et al., 2019):

$$Z_{eff} = \frac{\sum_i f_i A_i (\mu/\rho)_i}{\sum_i f_i \left(\frac{A_i}{Z_i}\right)(\mu/\rho)_i} \tag{4}$$

where A_i, f_i and Z_i represent the atomic weight, the fraction by mole of each constituent element of the glass and the atomic number, respectively.

Related mean free path (MFP), half value layer (HVL) and tenth value layer (TVL) protection parameters are related to the required thickness of the sample attenuating initial photon intensities to 50%, 10% and 36.8%, respectively. In order to indicate the mathematical clarification of aforementioned parameters, LAC can be easily related to ln2/μ, ln10/μ and 1/μ equations, respectively (Sharma et al., 2020; Kaçal et al., 2020).

Energy absorption build-up factor (EABF) and exposure build-up factor (EBF) values can be found utilizing both the equivalent atomic number (Z_{eq}) and geometric progression (G-P) fitting coefficients of the glasses. The detailed calculation procedures on EABF and EBF have been introduced in our previous works (Turhan et al., 2020; Sayyed et al., 2019).

Table 1
Chemical analysis and densities of the glasses under study.

	Expansion Borosilicate Glass	Borosilicate Glass (Clear)	Borosilicate Glass (Amber)	Expansion Soda-Lime Glass (Amber)	Expansion Soda-Lime Glass (Clear)
SiO_2	80.60%	75.00%	70.00%	67.00%	69.00%
B_2O_3	13.00%	10.50%	7.50%	5.00%	1.00%
Na_2O	4.00%	5.00%	6.50%	12.00%	13.00%
Al_2O_3	2.30%	7.00%	6.00%	7.00%	4.00%
CaO	–	1.50%	<1.0%	1.00%	5.00%
Fe_2O_3	–	–	1.00%	2.00%	–
TiO_2	–	–	5.00%	–	–
K_2O	–	–	1.00%	1.00%	3.00%
BaO	–	–	2.00%	<0.5%	2.00%
MnO_2	–	–	–	5.00%	–
MgO	–	–	–	–	3.00%
Density (g/cm^3)	2.23	2.34	2.42	2.50	2.50
Sample Code	G1	G2	G3	G4	G5

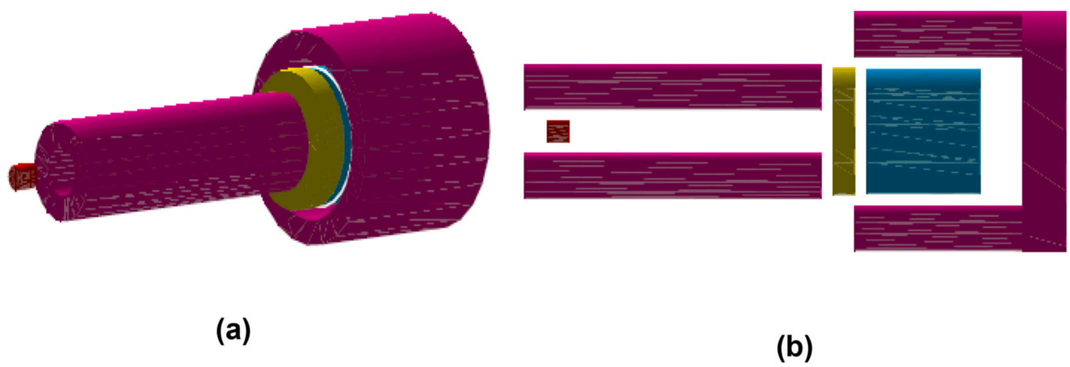

Fig. 1. Geometry and a general view of the simulation (Red is the radioactive point source. Purple is Pb shield collimator and blocks to minimize background and possible scattering. Green is the investigated glass sample. Blue shows the detection field).

2.2. Theoretical expectations and Monte Carlo simulations

In experimental studies, Monte Carlo simulations and theoretical expectations have significant meaning to have proper and complete discussions of the obtained outcomes. In some cases, it is possible to see that these two techniques are utilized to judge physicals phonemes when there is no chance to conduct experimental designs. In either way, the appropriate practice of the Monte Carlo simulations and theoretical expectations significantly contributes to the intended research and discussions. In the presented study, XCOM (Berger and Hubbell, 1987) program provides theoretical expectations for the proposed glass samples by using predefined elemental tables while Monte Carlo simulations of the gamma attenuation parameters are performed with help of FLUKA (Böhlen et al., 2014) and GEANT4 tools (Agostinelli et al., 2003). These three codes are well-known techniques in radiation shielding studies. In the process of the simulations, the glass samples are modeled in the FLUKA and GEANT4 codes, and the gamma radiations are simulated at the desired energies. Thus, let us to calculate the transmitted gamma radiation through the glass materials. The obtained numbers are inserted into the formula of the Lambert-Beer law, which provides the linear

Table 2
Comparisons of MAC values obtained by FLUKA, GEANT4, MATLAB and XCOM of G1 glasses.

MeV	G1						
	FLUKA	GEANT4	MATLAB	XCOM	RD_1	RD_2	RD_3
0.03	0.7899	0.7546	0.7669	0.7894	0.067	−2.625	−2.938
0.04	0.4309	0.4115	0.4281	0.4301	0.179	−0.765	−0.465
0.06	0.2409	0.2371	0.2420	0.2406	0.136	−0.082	0.585
0.08	0.1900	0.1843	0.1880	0.1885	0.775	−0.078	−0.292
0.1	0.1662	0.1654	0.1655	0.1655	0.432	−0.002	0.008
0.2	0.1259	0.1249	0.1255	0.1246	1.071	0.003	0.709
0.4	0.0960	0.0947	0.0870	0.0954	0.612	−0.007	−9.593
0.6	0.0802	0.0806	0.0806	0.0804	−0.260	0.002	0.213
0.8	0.0709	0.0709	0.0704	0.0705	0.570	0.003	−0.152
1	0.0632	0.0637	0.0634	0.0634	−0.269	0.002	0.016
2	0.0443	0.0444	0.0449	0.0445	−0.366	0.000	0.906
3	0.0364	0.0360	0.0363	0.0361	0.947	0.000	0.433
4	0.0314	0.0312	0.0316	0.0314	−0.105	−0.001	0.491
5	0.0286	0.0282	0.0284	0.0284	0.659	−0.001	0.004
6	0.0262	0.0261	0.0264	0.0263	−0.466	0.000	0.265
8	0.0238	0.0236	0.0238	0.0237	0.330	0.000	0.583
10	0.0224	0.0221	0.0222	0.0222	0.711	0.000	0.112
15	0.0204	0.0204	0.0205	0.0204	0.064	0.000	0.284

Table 3
Comparisons of MAC values obtained by FLUKA, GEANT4, MATLAB and XCOM of G2 glasses.

MeV	G2						
	FLUKA	GEANT4	MATLAB	XCOM	RD_1	RD_2	RD_3
0.03	0.8282	0.7988	0.8425	0.8280	0.024	−2.332	1.726
0.04	0.4478	0.4296	0.4443	0.4464	0.318	−0.723	−0.472
0.06	0.2454	0.2310	0.2459	0.2453	0.049	−0.331	0.240
0.08	0.1914	0.1857	0.1899	0.1905	0.453	−0.089	−0.313
0.1	0.1673	0.1662	0.1665	0.1665	0.463	−0.006	−0.001
0.2	0.1262	0.1209	0.1246	0.1247	1.156	−0.046	−0.053
0.4	0.0954	0.0951	0.0953	0.0954	0.051	−0.003	−0.131
0.6	0.0798	0.0802	0.0805	0.0803	−0.567	−0.001	0.287
0.8	0.0704	0.0708	0.0704	0.0705	−0.174	0.002	−0.209
1	0.0630	0.0637	0.0634	0.0633	−0.427	0.002	0.114
2	0.0441	0.0444	0.0444	0.0444	−0.728	0.000	0.068
3	0.0360	0.0359	0.0363	0.0361	−0.336	−0.001	0.436
4	0.0312	0.0313	0.0317	0.0314	−0.538	0.000	0.862
5	0.0282	0.0282	0.0284	0.0284	−0.621	0.000	0.127
6	0.0264	0.0262	0.0264	0.0264	0.005	−0.001	0.064
8	0.0238	0.0237	0.0239	0.0238	0.085	0.000	0.443
10	0.0219	0.0222	0.0223	0.0223	−1.956	0.000	0.045
15	0.0205	0.0205	0.0206	0.0205	−0.131	0.000	0.360

Table 4
Comparisons of MAC values obtained by FLUKA, GEANT4, MATLAB and XCOM of G3 glasses.

MeV	G3						
	FLUKA	GEANT4	MATLAB	XCOM	RD_1	RD_2	RD_3
0.03	1.1693	1.1408	1.1769	1.1750	−0.483	−3.902	0.163
0.04	0.9564	0.9126	0.9519	0.9575	−0.111	−4.097	−0.588
0.06	0.4175	0.3983	0.4212	0.4168	0.157	−0.737	1.043
0.08	0.2667	0.2567	0.2734	0.2678	−0.426	−0.284	2.051
0.1	0.2080	0.2000	0.2078	0.2077	0.158	−0.154	0.042
0.2	0.1312	0.1255	0.1300	0.1301	0.855	−0.058	−0.062
0.4	0.0968	0.0951	0.0957	0.0958	1.083	−0.006	−0.121
0.6	0.0805	0.0803	0.0804	0.0802	0.426	0.001	0.285
0.8	0.0694	0.0704	0.0708	0.0709	−2.212	−0.003	−0.158
1	0.0631	0.0635	0.0631	0.0631	−0.059	0.002	0.030
2	0.0444	0.0443	0.0443	0.0443	0.201	0.000	−0.056
3	0.0357	0.0359	0.0359	0.0361	−1.154	−0.001	−0.560
4	0.0312	0.0313	0.0315	0.0315	−1.047	−0.001	−0.016
5	0.0287	0.0284	0.0287	0.0286	0.271	0.000	0.181
6	0.0266	0.0265	0.0267	0.0267	−0.556	−0.001	0.064
8	0.0240	0.0241	0.0242	0.0242	−0.672	0.000	0.008
10	0.0229	0.0228	0.0229	0.0229	0.139	0.000	−0.149
15	0.0212	0.0213	0.0213	0.0213	−0.371	0.000	0.159

Table 5
Comparisons of MAC values obtained by FLUKA, GEANT4, MATLAB and XCOM of G4 glasses.

MeV	G4						
	FLUKA	GEANT4	MATLAB	XCOM	RD_1	RD_2	RD_3
0.03	1.1831	1.1831	1.2410	1.2180	−2.948	−8.197	1.850
0.04	0.6891	0.6891	0.7046	0.7087	−2.840	−3.795	−0.576
0.06	0.3221	0.3221	0.3219	0.3287	−2.052	−0.781	−2.103
0.08	0.2240	0.2240	0.2258	0.2268	−1.242	−0.393	−0.423
0.1	0.1847	0.1847	0.1854	0.1854	−0.370	−0.143	0.026
0.2	0.1274	0.1274	0.1268	0.1268	0.435	−0.060	−0.006
0.4	0.0958	0.0958	0.0952	0.0953	0.495	0.006	−0.065
0.6	0.0802	0.0802	0.0803	0.0801	0.071	0.000	0.244
0.8	0.0696	0.0696	0.0701	0.0702	−0.839	0.002	−0.163
1	0.0630	0.0630	0.0631	0.0631	−0.128	0.003	0.010
2	0.0442	0.0442	0.0443	0.0443	−0.276	−0.001	−0.036
3	0.0358	0.0358	0.0359	0.0361	−0.802	−0.001	−0.543
4	0.0312	0.0312	0.0315	0.0315	−0.948	0.000	−0.006
5	0.0285	0.0285	0.0287	0.0286	−0.465	−0.001	0.192
6	0.0265	0.0265	0.0267	0.0267	−0.797	0.000	0.075
8	0.0240	0.0240	0.0242	0.0242	−0.743	0.000	0.029
10	0.0230	0.0230	0.0229	0.0229	0.401	0.000	−0.122
15	0.0211	0.0211	0.0213	0.0213	−0.840	0.000	0.000

Table 6
Comparisons of MAC values obtained by FLUKA, GEANT4, MATLAB and XCOM of G5 glasses.

MeV	G5						
	FLUKA	GEANT4	MATLAB	XCOM	RD_1	RD_2	RD_3
0.03	1.1572	1.1142	1.0741	1.0860	6.155	3.142	−1.110
0.04	0.9484	0.8991	0.9495	0.9600	−1.221	−5.480	−1.104
0.06	0.4146	0.4000	0.4064	0.4163	−0.415	−0.653	−2.440
0.08	0.2658	0.2552	0.2663	0.2678	−0.764	−0.322	−0.551
0.1	0.2079	0.1942	0.2080	0.2078	0.043	−0.264	0.075
0.2	0.1311	0.1262	0.1303	0.1303	0.582	−0.051	−0.011
0.4	0.0964	0.0948	0.9495	0.096	0.393	−0.011	−1.104
0.6	0.0805	0.0804	0.0806	0.0804	0.097	0.000	0.254
0.8	0.0700	0.0701	0.0703	0.0704	−0.640	−0.002	−0.168
1	0.0632	0.0635	0.0633	0.0632	0.056	0.002	0.085
2	0.0441	0.0448	0.0448	0.0444	−0.572	0.002	0.961
3	0.0361	0.0360	0.0360	0.0362	−0.336	−0.001	−0.519
4	0.0318	0.0311	0.0316	0.0317	0.203	−0.002	−0.250
5	0.0290	0.0289	0.0288	0.0288	0.824	0.000	−0.031
6	0.0268	0.0266	0.0269	0.0268	0.010	−0.001	0.264
8	0.0247	0.0249	0.0244	0.0244	1.127	0.001	−0.074
10	0.0231	0.0229	0.0231	0.0231	−0.030	0.000	−0.143
15	0.0218	0.0218	0.0217	0.0216	0.813	0.000	0.351

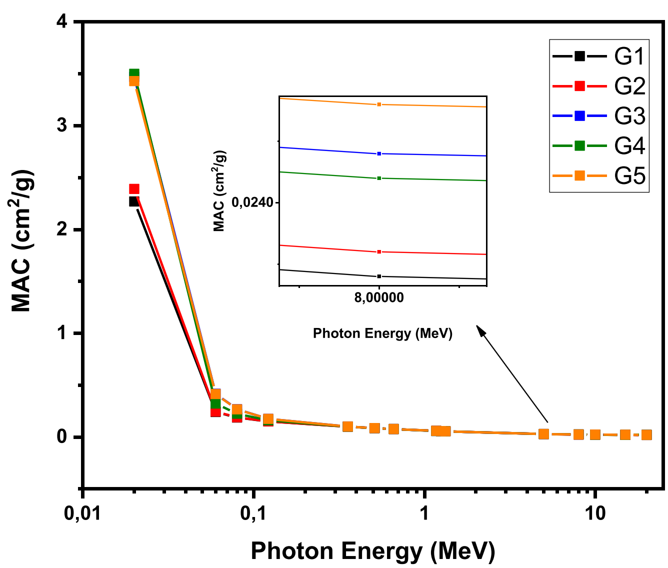

Fig. 2. Mass attenuation coefficients (MACs) of the chosen glasses with photon energy from 0.03 to 15 MeV.

attenuation coefficient for the chosen energy and material at a certain shield thickness. Exactly same gamma energy values are chosen in FLUKA, GEANT4 and XCOM steps, in order to make proper and accurate comparisons between different research tools.

3. Results and discussions

The results presented in Table 1 have been used to provide a detailed assessment of gamma ray shielding performance. The chemical analyses and densities of the expansion borosilicate glass (G1), borosilicate glass (clear) (G2), borosilicate glass (amber) (G3), expansion soda-lime glass (amber) (G4), and expansion soda-lime glass (clear) (G5) samples are shown in the table. The theoretical mass attenuation coefficients (MAC) of borosilicate based glasses containing different amounts of Na_2O, Al_2O_3, CaO, Fe_2O_3, TiO_2, K_2O, BaO, MnO_2 and MgO are determined as a function of photon energy with help of mixture rule based WinXCom program while the simulation numbers are estimated by detecting the photons that passes through the glasses through a narrow beam transmission (Fig. 1) designed in FLUKA and GEANT4 Monte Carlo simulation codes as well as MATLAB code for a wide photon energy region of 0.03–15 MeV. The detailed comparisons of theoretical and simulation values can be found in Tables 2–5 and 6. The relative deviations (RD,%) among FLUKA, GEANT4, MATLAB code and XCOM theoretical MAC results were further calculated through the following relation:

$$RD = \left(\frac{MAC_{1,2,3} - MAC_{theoretical}}{MAC_{1,2,3}}\right) * 100 \quad (11)$$

where $MAC_{1,2,3}$ donates mass attenuation coefficients estimated by FLUKA, GEANT4 MATLAB code, respectively.

Tables 2–6 represents the harmony of theoretical and simulation methods in the MAC of the borosilicate glasses. The obtained RD values in Tables 2–5 and **6** are found to be in the range of <10% for FLUKA-XCOM, GEANT4-XCOM, MATLAB-XCOM results. These consistencies are quite clear that the obtained MAC results of the glasses are in good agreement with each other and related shielding parameters of the examined G1-G5 glasses are obtained with high accuracy. The arisen differences can be attributed to the mixture rule that disregards the interactions among atoms in a mixture composite.

The calculated MAC values for all the borosilicate glasses have been displayed in Fig. 2. This figure clearly exhibits that the MAC values of various borosilicate glasses are decreased with the increase of photon energy. Regardless of having any additions, the MAC reduces

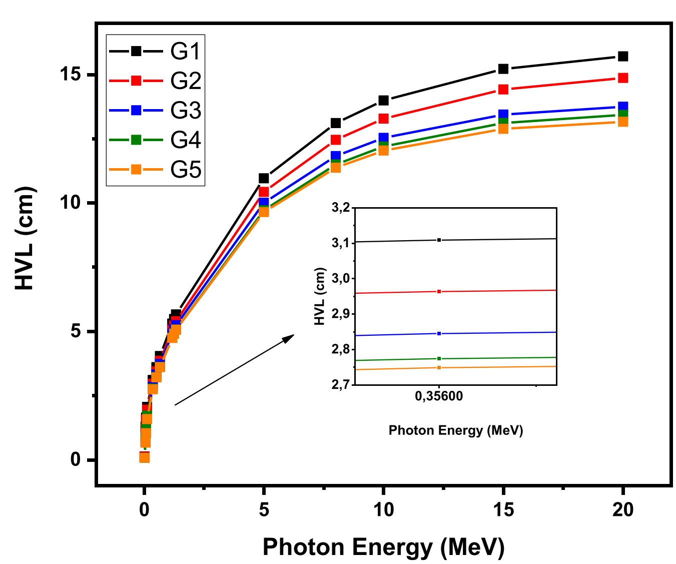

Fig. 3. HVLs of the chosen glasses with photon energy from 0.03 to 15 MeV.

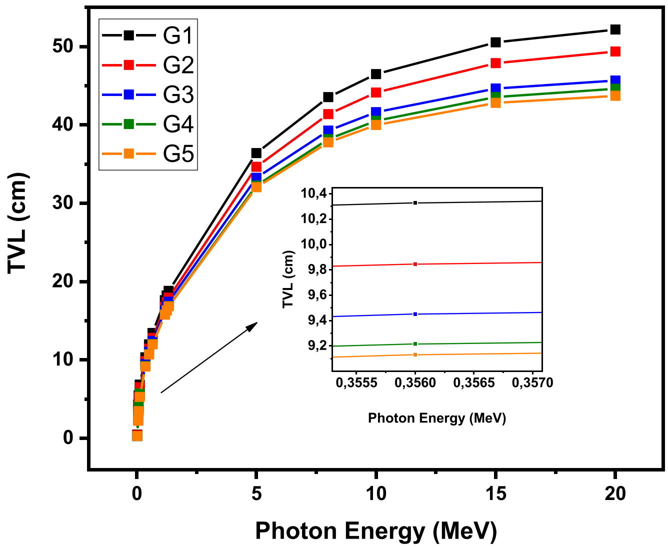

Fig. 4. TVLs of the chosen glasses with photon energy from 0.03 to 15 MeV.

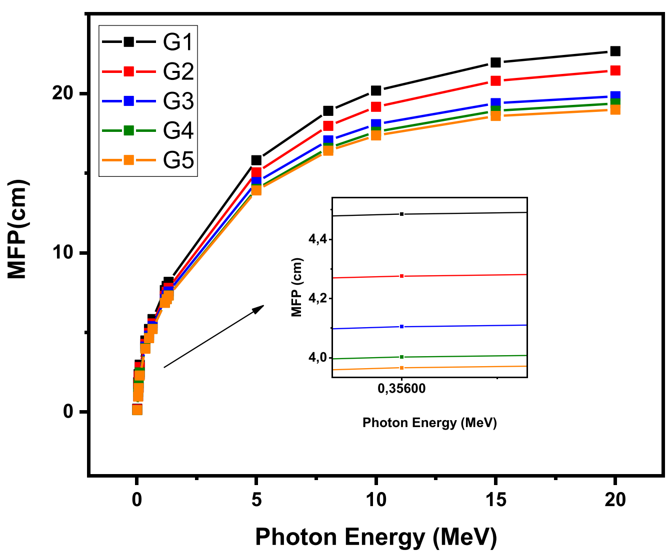

Fig. 5. MFPs of the chosen glasses with photon energy from 0.03 to 15 MeV.

exponentially over about 0.4 MeV. The reason of the rapid variation at low-level energies results from the photoelectric effect's (PE) dominant role, where its cross sections are related to Z^{4-5} and also, inversely proportional incident photon energy given as $E^{3.5}$. Additionally, the pair production (PP) mode is the dominant in higher energy region (3<E<15 MeV), where PP's cross-section changes with Z^2; therefore, a slight increase in the MAC values was observed. On the other hand, in 0.4<E<3 MeV energy region, the presented decrease goes on as a linear line with the gamma energy increase. This difference is due to the Compton scattering (CS) mode which is interaction mechanism of the incident photon with the matter. This mode is in general more effective mechanism at medium energies, due to that CS's cross-section is associated with the energy as E^{-1} and atomic number as Z. Moreover, the present data on MAC parameter are supported by the findings published on 10 TeO2–10CdO-(20+x) PbO-(60-x) B2O3 (where x = 10, 15, 20, 25, 30 mol% respectively) (Alotaibi et al., 2021)and (49-x) B2O3–35TeO2–15PbO-1.0Y2O3-xNd2O3 (where x = 0.0, 0.5, 1.0, 1.5, 2.0, and 2.5% mol) (Tekin et al., 2021).

The theoretical HVL, TVL, and MFP values versus the photon energy were illustrated in Figs. 3, 4 and 5. The comparison of the shielding

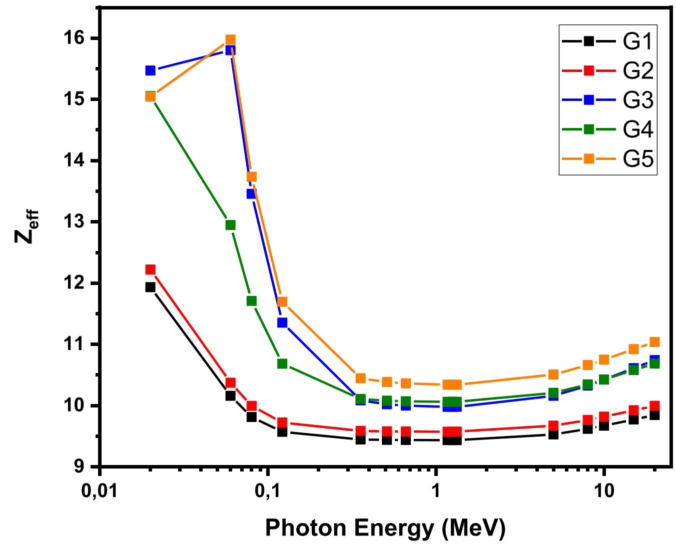

Fig. 6. Z_{eff} values of the chosen glasses with photon energy from 0.03 to 15 MeV.

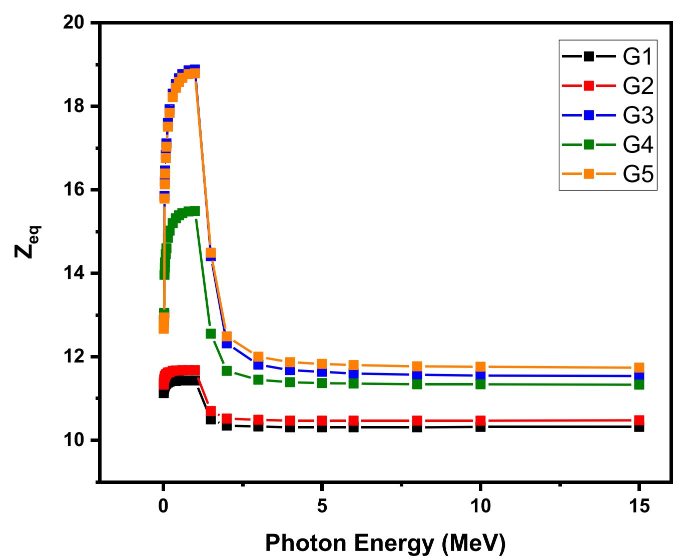

Fig. 7. Z_{eq} values of the chosen glasses with photon energy from 0.03 to 15 MeV.

effectiveness for the borosilicate glasses including different proportions of various content is quite enlightening. All HVL, TVL, and MFP values increase with the gamma radiation energy increase while all decrease with the increase of dopant amount: G5<G4<G3<G2<G1. While these parameters are independent of the glasses composition at low energies, borosilicate-based glasses have smaller MFP, HVL, and TVL values at medium energies. Also, the variations on MFPs, HVLs and TVLs depending on chemical composition in glasses are quite remarkable at about 10–20 MeV. It means that the replacement of Ca, Fe, and Ba contents with B and Si chemicals, which leads to increase in the glass densities, implies a superior shielding absorber for the required thickness. The similar variation in these parameters is explained by the replacement in $xTiO_2$-$xCeO_2$-(30-x) PbO-(70-x) B_2O_3 where 2 ≤x ≤ 10 mol% (G. P. Singh et al., 2021, 2) and in TeO_2–ZnO–Nb_2O_5–Gd_2O_3 which publish similar findings estimated through Phy-X/PSD software (Al-Hadeethi et al., 2020).

Determination of Z_{eff} values for any material attributes to the possibilities of high energetic photon interactions with this material. In this

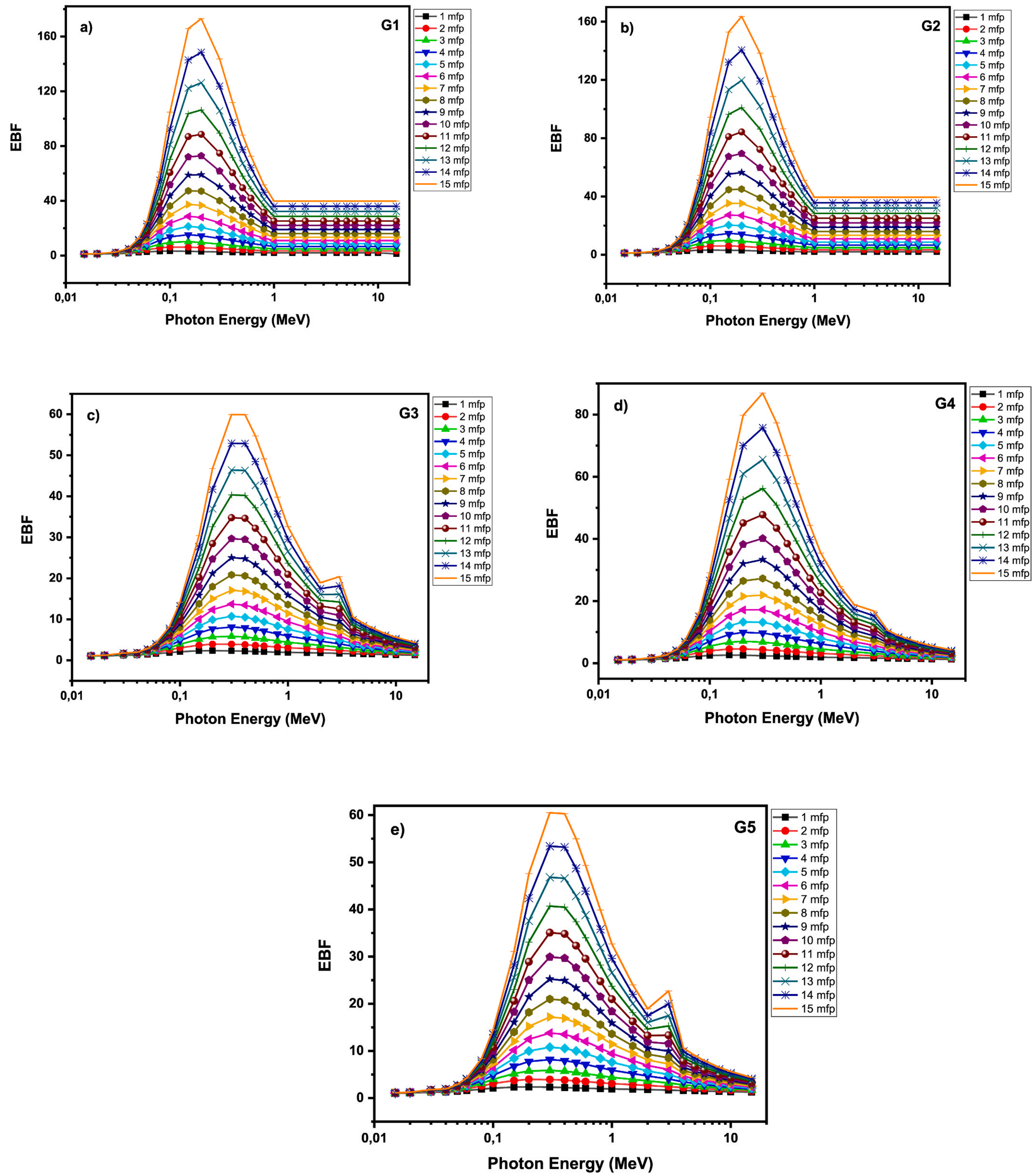

Fig. 8. The exposure buildup factors in the energy region 0.03–15 MeV at 1–15 mfp.

context, the Z_{eff} results of borosilicate-based glass systems against photon energies of 0.03 – 15 MeV have been estimated and represented in Fig. 6. According to this figure, change in Z_{eff} values of glasses is in the descending order of G5>G4>G3>G2>G1 and G5>G3>G4>G2>G1 for high and low energies, respectively. Thus, G5 system among the investigated borosilicate glasses has the highest Z_{eff} value over a wide photon energy region. Its high Z_{eff} can be referred to as its amount (2%) of Ba content as given in Table 1 and thus, it means to have larger interaction of incident photons with G5 glass as compared to G4, G3, G2, and G1 glasses. The photon abruptly loses their energies together with this interaction and minimizes the penetrating of the photons across G5.

Besides, EBF plays an important role in shielding designs, radiation therapy, and dosimetry purposes (Kara et al., 2020; Kara et al., 2020). The estimated equivalent atomic numbers (Z_{eq}) and EBF values for G1,

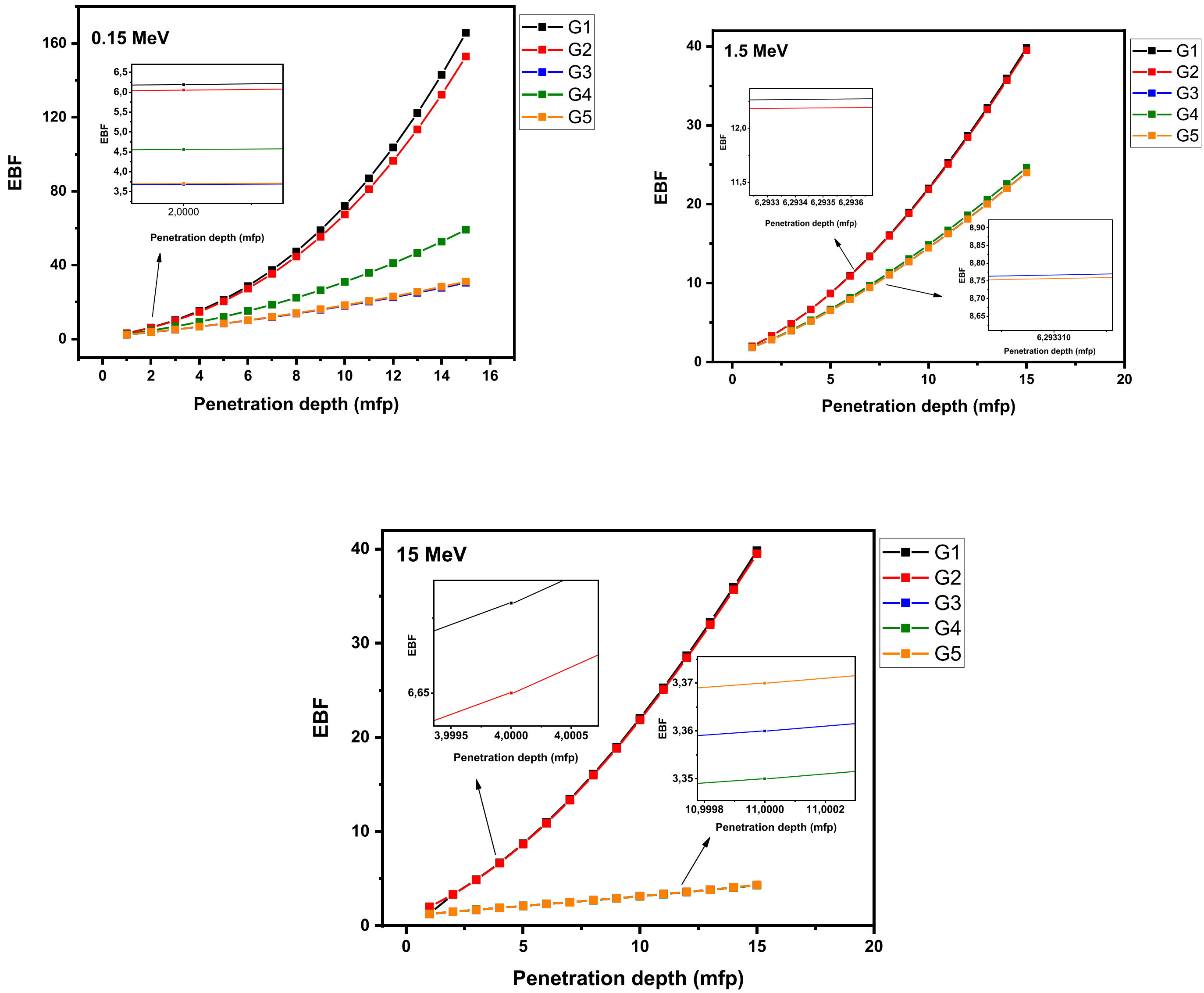

Fig. 9. The exposure buildup factors in the penetration depths at 0.15, 1 and 15 MeV.

G2, G3, G4, and G5 glasses in the energy range of 0.03–15 MeV corresponding to the chosen penetration depths (1–15 MFP) were calculated using G-P fitting approach and shown in Fig. 7 and **8(a-e)**. Also, the changes of EBF depending on penetration depths at 0.15, 1.5, and 15 MeV are graphically demonstrated in Fig. 9. It was observed that at low, intermediate and high photon energies, the EBF for glasses possesses a Gaussian-like distribution. Parallel to MAC parameters, the EBF trend in Fig. 8 (a-e) can be clarified by partial photon interaction mechanisms. For the low energy values, photons are removed or absorbed while the PE mechanism is dominant and hence, the scattering probability is very small. Thereafter, the peak region of Gaussian-like distribution is related to the increase in photon energy and due to the fact that CS dominates over these energies, leading to a higher proportion of multiple scattering instead of absorption. It gives rise to a reduction of photon energy without complete removal of the photon, thus the larger EBF values can be observed at the moderate energy values. The pair production process at high energies is the proponent and the EBF values gradually decrease with the incident photon energy.

4. Conclusions

The MACs of various borosilicate glasses were estimated using FLUKA, GEANT4, and MATLAB simulation codes. The obtained results were further validated with help of XCOM software. The insertion of BaO in the G5 sample leads to an increase in both MAC and Z_{eff} values while reducing MFPs, HVLs and TVLs. G5 sample which has the maximum Z amount such as BaO has better photon attenuation performance than the others in the sample. Finally, glasses that are transparent to visible light may be offered for usage at nuclear research centers, nuclear reactors, and oncology departments in hospitals where radiation zones exist.

Author statement

O. Kilicoglu: Data Collection, Supervision, Validation, and writing.
F. Akman: Validation, and writing.
H. Ogul: Validation, and writing.
O. Agar: Data Collection, Validation, and writing.
U. Kara: Monte Carlo Simulation.

Declaration of competing interest

The authors declare that they have no known competing financial interests or personal relationships that could have appeared to influence the work reported in this paper.

Data availability

No data was used for the research described in the article.

References

Agostinelli, Sea, Allison, John, al Amako, K., Apostolakis, John, Araujo, H., Arce, Pedro, Asai, Makoto, Axen, D., Banerjee, Swagato, Gjni Barrand, 2003. GEANT4-a simulation toolkit. Nucl. Instrum. Methods Phys. Res. Sect. A Accel. Spectrom. Detect. Assoc. Equip. 506 (3), 250–303.

Akkurt, Iskender, Gunoglu, Kadir, Kurtuluş, Recep, Kavas, Taner, 2021. X-ray shielding parameters of lanthanum oxide added waste soda-lime glass. X Ray Spectrom. 50 (3), 168–179.

Akman, F., Kaçal, M.R., Sayyed, M.I., Karataş, H.A., 2019. Study of gamma radiation attenuation properties of some selected ternary alloys. J. Alloys Compd. 782, 315–322.

Akman, Ferdi, Ozkan, I., Kaçal, Mustafa Recep, Polat, Hasan, Shams, AM Issa, Tekin, H. O., Agar, O., 2021. Shielding features, to non-ionizing and ionizing photons, of FeCr-based composites. Appl. Radiat. Isot. 167, 109470.

Al-Hadeethi, Y., Sayyed, M.I., 2019. Analysis of borosilicate glasses doped with heavy metal oxides for gamma radiation shielding application using Geant4 simulation code. Ceram. Int. 45 (18), 24858–24864.

Al-Hadeethi, Y., Sayyed, M.I., Agar, O., 2020. Ionizing photons attenuation characterization of quaternary tellurite-zinc-niobium-gadolinium glasses using phy-X/PSD software. J. Non-Cryst. Solids 538, 120044.

Alotaibi, B.M., Alotiby, Mohammed, Kumar, Ashok, Mahmoud, K.A., Sayyed, M.I., Al-Yousef, Haifa A., Al-Hadeethi, Y., 2021. Gamma-ray shielding, physical, and structural characteristics of TeO2-CdO-PbO-B2O3 glasses. Opt. Mater. 119, 111333.

Alwaeli, Mohamed, 2017. Investigation of gamma radiation shielding and compressive strength properties of concrete containing scale and granulated lead-zinc slag wastes. J. Clean. Prod. 166, 157–162.

Azeez, Mukhtar Oluwaseun, Ahmad, Shamsad, Salah, U., Al-Dulaijan, Maslehuddin, Mohammed, Naqvi, Akhtar Abbas, 2019. Radiation shielding performance of heavy-weight concrete mixtures. Construct. Build. Mater. 224, 284–291.

Baalamurugan, J., Ganesh Kumar, V., Chandrasekaran, S., Balasundar, S., Venkatraman, B., Padmapriya, R., Bupesh Raja, V.K., 2019. Utilization of induction furnace steel slag in concrete as coarse aggregate for gamma radiation shielding. J. Hazard Mater. 369, 561–568.

Berger, Martin J., Hubbell, J.H., 1987. XCOM: Photon Cross Sections on a Personal Computer. National Bureau of Standards, Washington, DC (USA) (Center for Radiation …).

Böhlen, T.T., Cerutti, Francesco, Chin, M.P.W., Fassò, Alberto, Ferrari, Alfredo, Garcia Ortega, P., Mairani, Andrea, Sala, Paola R., Smirnov, George, Vlachoudis, Vasilis, 2014. The FLUKA code: developments and challenges for high energy and medical applications. Nucl. Data Sheets 120, 211–214.

Boukhris, Imed, Al-Buriahi, M.S., Akyildirim, Hakan, Alalawi, Amani, Kebaili, Imen, Sayyed, M.I., 2020. Chalcogenide glass-ceramics for radiation shielding applications. Ceram. Int. 46 (11), 19385–19392.

Cherkashina, N.I., Pavlenko, V.I., Noskov, A.V., 2019. Radiation shielding properties of polyimide composite materials. Radiat. Phys. Chem. 159, 111–117.

Issa, Shams A.M., Saddeek, Yasser B., Sayyed, M.I., Tekin, H.O., Kilicoglu, Ozge, 2019. Radiation shielding features using MCNPX code and mechanical properties of the PbONa2OB2O3CaOAl2O3SiO2 glass systems. Compos. B Eng. 167 (June), 231–240. https://doi.org/10.1016/j.compositesb.2018.12.029.

Kacal, Mustafa R., Akman, Ferdi, Sayyed, M.I., 2019. Investigation of radiation shielding properties for some ceramics. Radiochim. Acta 107 (2), 179–191.

Kaçal, Mustafa Recep, Polat, Hasan, Oltulu, M., Akman, Ferdi, Agar, O., Tekin, H.O., 2020. Gamma shielding and compressive strength analyses of polyester composites reinforced with zinc: an experiment, theoretical, and simulation based study. Appl. Phys. A 126 (3), 1–15.

Kara, Umit, Kilicoglu, Ozge, Ersoy, Sıddıka, 2020a. Structural and gamma-ray attenuation coefficients of different OAD films for nuclear medicine applications. Radiat. Phys. Chem. 172 (July), 108785 https://doi.org/10.1016/j.radphyschem.2020.108785.

Kara, Umit, Kilicoglu, Ozge, Karaibrahimoglu, Adnan, Cavdarli, Kemal, Ince, Fuat, 2020b. Radiation attenuation properties of removable partial dentures (RPD). Mater. Chem. Phys. 253 (October), 123301 https://doi.org/10.1016/j.matchemphys.2020.123301.

Kavas, Taner, Kurtulus, Recep, Mahmoud, K.A., Sayyed, M.I., Akkurt, Iskender, Gunoglu, Kadir, 2021. Radiation shielding competencies for waste soda-lime-silicate glass reinforced with Ta2O5: experimental, computational, and simulation studies. Appl. Phys. A 127 (3), 1–14.

Kavaz, Esra, Ekinci, Neslihan, Tekin, H.O., Sayyed, M.I., Aygün, B., Perişanoğlu, U., 2019. Estimation of gamma radiation shielding qualification of newly developed glasses by using WinXCOM and MCNPX code. Prog. Nucl. Energy 115, 12–20.

Kilicoglu, Ozge, 2019. Characterization of copper oxide and cobalt oxide substituted bioactive glasses for gamma and neutron shielding applications. Ceram. Int. 45 (17), 23619–23631. https://doi.org/10.1016/j.ceramint.2019.08.073. Part B).

Kurtulus, Recep, Kavas, Taner, Akkurt, Iskender, Gunoglu, Kadir, 2020. An experimental study and WinXCom calculations on X-ray photon characteristics of Bi2O3-and Sb2O3-added waste soda-lime-silica glass. Ceram. Int. 46 (13), 21120–21127.

Kurtulus, Recep, Kavas, Taner, Akkurt, Iskender, Gunoglu, Kadir, Tekin, H.O., Kurtulus, Cansu, 2021. A comprehensive study on novel alumino-borosilicate glass reinforced with Bi2O3 for radiation shielding applications: synthesis, spectrometer, XCOM, and MCNP-X works. J. Mater. Sci. Mater. Electron. 32 (10), 13882–13896.

Kurudirek, Murat, Chutithanapanon, Natsupon, Laopaiboon, Raewat, Yenchai, Chadet, Bootjomchai, Cherdsak, 2018. Effect of Bi2O3 on gamma ray shielding and structural properties of borosilicate glasses recycled from high pressure sodium lamp glass. J. Alloys Compd. 745, 355–364.

Limkitjaroenporn, P., Kaewkhao, J., Limsuwan, P., Chewpraditkul, W., 2011. Physical, optical, structural and gamma-ray shielding properties of lead sodium borate glasses. J. Phys. Chem. Solid. 72 (4), 245–251.

More, Chaitali V., Zainab, Alsayed, Mohamed, Badawi, Abouzeid, Thabet, Pawar, Pravina P., 2021. Polymeric composite materials for radiation shielding: a review. Environ. Chem. Lett. 19 (3), 2057–2090.

Oto, Berna, Kavaz, Esra, Durak, Halil, Aras, Aydın, Madak, Zekiye, 2019. Effect of addition of molybdenum on photon and fast neutron radiation shielding properties in ceramics. Ceram. Int. 45 (17), 23681–23689.

Ruengsri, S., Insiripong, S., Sangwaranatee, N., Kaewkhao, J., 2015. Development of barium borosilicate glasses for radiation shielding materials using rice husk ash as a silica source. Prog. Nucl. Energy 83, 99–104.

Sangwaranatee, N., Cheewasukhanont, W., Limkitjaroenporn, P., Borisut, P., Wongdamnern, N., Khrongchaiyaphum, F., Kothan, S., Kaewkhao, J., 2021. Development of bismuth alumino borosilicate glass for radiation shielding material. Radiat. Phys. Chem. 186, 109542.

Sayyed, M.I., Mahmoud, K.A., Tashlykov, O.L., Khandaker, Mayeen Uddin, Faruque, M. R.I., 2020. Enhancement of the shielding capability of soda-lime glasses with Sb2O3 dopant: a potential material for radiation safety in nuclear installations. Appl. Sci. 11 (1), 326.

Sayyed, M.I., Tekin, H.O., Agar, O., 2019. Gamma photon and neutron attenuation properties of MgO-BaO-B2O3-TeO2-Cr2O3 glasses: the role of TeO2. Radiat. Phys. Chem. 163, 58–66.

Sharma, Amandeep, Sayyed, M.I., Agar, O., Kaçal, M.R., Polat, H., Akman, F., 2020. Photon-shielding performance of bismuth oxychloride-filled polyester concretes. Mater. Chem. Phys. 241, 122330.

Singh, Gurinder Pal, Singh, Joga, Kaur, Parvinder, Singh, Taminder, Kaur, Ravneet, Kaur, Simranpreet, Singh, D.P., 2021. Impact of TiO2 on radiation shielding competencies and structural, physical and optical properties of CeO2-PbO-B2O3 glasses. J. Alloys Compd. 885, 160939.

Singh, Vishwanath P., Badiger, N.M., Chanthima, N., Kaewkhao, J., 2014. Evaluation of gamma-ray exposure buildup factors and neutron shielding for bismuth borosilicate glasses. Radiat. Phys. Chem. 98, 14–21.

Tekin, H.O., Shams, AM Issa, Ahmed, Emad, Rammah, Y.S., 2021. The impact of Nd3+ ions on linear/nonlinear and the ionizing radiation attenuation parameters of TeO2-PbO-Y2O3 glasses. J. Mater. Sci. Mater. Electron. 32 (13), 17200–17219.

Tekin, H.O., Kavaz, E., Altunsoy, E.E., Kilicoglu, O., Agar, O., Erguzel, T.T., Sayyed, M.I., 2019. An extensive investigation on gamma-ray and neutron attenuation parameters of cobalt oxide and nickel oxide substituted bioactive glasses. Ceram. Int. 45 (8), 9934–9949. https://doi.org/10.1016/j.ceramint.2019.02.036.

Tekin, H.O., Kilicoglu, O., 2020. The influence of gallium (Ga) additive on nuclear radiation shielding effectiveness of Pd/Mn binary alloys. J. Alloys Compd. 815 (January), 152484 https://doi.org/10.1016/j.jallcom.2019.152484.

Tellili, Borhan, Elmahroug, Youssef, Souga, Chedly, 2017. Investigation on radiation shielding parameters of cerrobend alloys. Nucl. Eng. Technol. 49 (8), 1758–1771.

Tijani, S.A., Kamal, Salahuddin M., Al-Hadeethi, Y., Arib, Mehenna, Hussein, M.A., Wageh, S., Dim, L.A., 2018. Radiation shielding properties of transparent erbium zinc tellurite glass system determined at medical diagnostic energies. J. Alloys Compd. 741, 293–299.

Tishkevich, D.I., Grabchikov, S.S., Grabchikova, E.A., Vasin, D.S., Lastovskiy, S.B., Yakushevich, A.S., Vinnik, D.A., Zubar, T.I., Kalagin, I.V., Mitrofanov, S.V., 2020. Modeling of paths and energy losses of high-energy ions in single-layered and multilayered materials. In: IOP Conference Series: Materials Science and Engineering, vol. 848. IOP Publishing, 012089.

Tishkevich, D.I., Grabchikov, S.S., Lastovskii, S.B., Trukhanov, S.V., Zubar, T.I., Vasin, D. S., Trukhanov, A.V., 2018. Correlation of the synthesis conditions and microstructure for Bi-based electron shields production. J. Alloys Compd. 749, 1036–1042.

Turhan, Mehmet Fatih, Akman, Ferdi, Polat, Hasan, Kaçal, Mustafa Recep, Demirkol, İskender, 2020. Gamma-ray attenuation behaviors of hematite doped polymer composites. Prog. Nucl. Energy 129, 103504.

Zakaly, Hesham MH., Saudi, H.A., Shams, AM Issa, Rashad, M., Elazaka, A.I., Tekin, H. O., Saddeek, Y.B., 2021. Alteration of optical, structural, mechanical durability and nuclear radiation attenuation properties of barium borosilicate glasses through BaO reinforcement: experimental and numerical analyses. Ceram. Int. 47 (4), 5587–5596.